

Simultaneous reconstruction of absorption and scattering images by multichannel measurement of purely temporal data

Jeremy C. Hebden, Florian E. W. Schmidt, Martin E. Fry, Martin Schweiger,
Elizabeth M. C. Hillman, and David T. Delpy

Department of Medical Physics, University College London, 11-20 Capper Street, London WC1E 6JA, UK

Simon R. Arridge

Department of Computer Science, University College London, Gower Street, London WC1E 6BT, UK

Received December 10, 1998

We present what is believed to be the first simultaneous reconstruction of the internal scattering and absorbing properties of a highly scattering medium by use of purely temporal data. These results are also the first acquired with the multichannel time-resolved imaging system developed at University College London.

© 1999 Optical Society of America

OCIS codes: 170.3010, 170.3890, 170.6920, 170.6960.

Potential clinical applications such as the diagnosis of abnormalities in the infant brain are motivating considerable effort in the development of imaging techniques based on the detection of transmitted optical radiation.^{1,2} The general principle on which optical tomography is based is that a finite set of measurements of transmitted light between pairs of points on the surface of an object is sufficient for reconstruction of an arbitrary three-dimensional (3D) distribution of internal scatterers and absorbers. Unfortunately the predominance of scatter prevents the use of the Radon transform and the backprojection methods for all but a limited set of circumstances.² A more productive approach to imaging is to determine the parameters that describe an appropriate model of photon transport within the investigated medium by comparing its predictions with the measured data. The model is then adjusted iteratively until acceptable correspondence is achieved: convergence toward the correct solution is assisted by the use of appropriate regularization methods. This technique requires three distinct components: a forward model that can generate a set of reliable measurements from a given internal two-dimensional (2D) or 3D distribution of scattering and absorbing parameters; the definition of an objective function to be minimized, based on the error between model predictions and experimental data; and a scheme for adjusting the parameters of the forward model so that minimization is achieved.

The image reconstruction scheme employed at University College London (UCL), known as temporal optical absorption and scattering tomography (TOAST), uses a finite-element method forward model and an iterative reconstruction algorithm.³ We originally proposed a Levenberg–Marquardt algorithm combined with a secondary basis to reduce the dimensionality of the problem and image filtering during reconstruction to reduce artifacts.⁴ This algorithm, adapted to the frequency domain, has been extensively studied by other researchers.^{5–7} More recently we have intro-

duced gradient-based methods that have been found to be significantly faster.⁸

In principle, iterative imaging schemes can utilize external measurements of any type. However, absolute measurements of transmitted intensity across several centimeters of tissue are much more strongly influenced by photon interactions at the surface than by the specific optical properties of localized regions deeper within the tissue. This finding has been confirmed by a sensitivity analysis.⁹ Consequently, there has been a considerable effort to pursue alternative data types that are independent of total intensity and that have greater sensitivity to structure of tissues deep below the surface. This effort has led researchers toward the development of instruments that perform measurements in the time or the frequency domain. The former measure the temporal distribution of photons transmitted between points on the surface in response to illumination by an impulse of light, whereas the latter determine the modulation amplitude and phase delay in response to an intensity-modulated signal. Although frequency-domain systems are generally less expensive and easier to develop, current technology gives the time domain a significant advantage in terms of effective temporal resolution and available source intensity.

The majority of the reported results in optical tomography are for relative, or dynamic, imaging, in which measurements are acquired at two different states and difference data are employed in the reconstruction.^{7,10} In addition, many results are for either absorption-only or scatter-only images. The reason for this stems from a fundamental nonuniqueness of the diffusion approximation such that simultaneous reconstruction always exhibits cross talk unless absorption and scatter perturbations are located at the same point.¹¹ The use of complex data in the Fourier domain allows the separation of two variables, and taking the logarithm of the intensity difference eliminates uncertainty in the absolute amplitude.

Absolute imaging by use of intensity measurements has been reported by Jiang *et al.*,⁵ but their method required calibration on a uniform object with the same background optical properties minus the internal features. The output of their finite-element method forward model, adjusted to fit the calibration object, effectively takes the place of a reference measurement. Results obtained with this method have been applied to the special case in which the absorption and scatter profiles of the image were exactly correlated,^{5,6} and so cross talk was not apparent. Absolute imaging without use of a reference measurement has been reported by Ueda *et al.*,¹² who reconstructed only absorption images from intensity information.

At UCL we have built an optical imaging device that attempts to gain as much information as current technology allows, based on the principle that one cannot do better than detect every transmitted photon and measure its flight time with the highest possible temporal resolution. The result is a 32-channel time-resolved system based on state-of-the-art time-correlated single-photon-counting instrumentation. The system, described in detail elsewhere,¹³ is illustrated schematically in Fig. 1. Picosecond pulses from a Ti:sapphire laser are coupled successively into a series of optical fibers so that the point of illumination on the tissue surface is varied sequentially. Meanwhile the transmitted light is collected by 32 detector fiber bundles, 2.5 mm in diameter, simultaneously. The source and the detector fibers are arranged at regular intervals around the circumference of the patient. Each of the 32 detector fiber bundles is coupled to the cathode of a microchannel plate-photomultiplier tube (MCP-PMT) via a variable optical attenuator. The attenuators ensure that the intensity of detected light does not saturate or damage the MCP-PMT, and the flux of photons is sufficiently small to prevent detection of multiple photons during each electronic cycle. The system employs four 8-anode MCP-PMT's. Electronic pulses generated each time a photon is detected are sampled by a sophisticated electronic system manufactured by EG&G Ortec. By measurement of the delay between these pulses and a reference signal received directly via the laser, histograms of photon flight times (known as temporal point-spread functions) are built up within the storage memory of the device. The imaging instrument is known as the multichannel optoelectronic near-infrared system for time-resolved image reconstruction (MONSTIR).

For the first significant test of the MONSTIR, a solid-tissue-equivalent phantom was constructed in the form of a cylindrical block, 85 mm in length and 70 mm in diameter, as illustrated in Fig. 2. The phantom is made from epoxy resin mixed with appropriate concentrations of titanium dioxide particles and near-infrared dye to provide a transport scatter coefficient of $\mu_s' = 1.0 \pm 0.02 \text{ mm}^{-1}$ and an absorption coefficient $\mu_a = 0.01 \pm 0.002 \text{ mm}^{-1}$ at a wavelength of 800 nm. The refractive index is 1.56. Embedded along the length of the phantom are three regions with coefficients having the following relative values: A, $5\mu_s'$ and μ_a ; B, μ_s' and $5\mu_a$; and C, $2\mu_s'$ and $2\mu_a$. Each region is 8 mm in diameter and is located 15 mm from the central axis

of the phantom. A black plastic ring was constructed to fit around the circumference of the phantom and to hold 32 detector fiber bundles and 32 source fibers in contact with the surface. However, for this initial validation experiment only eight detector bundles, connected to a single MCP-PMT, and only two source fibers were employed. The ring was rotated around the phantom to collect data at 16 detector positions for each of 16 source positions. The outcome of our acquisition protocol was to place sources at 22.5° intervals around the circumference, and for each source position the 16 detectors are effectively arranged at 11.25° intervals on the half-circumference immediately opposite each source. This fan-beam arrangement, illustrated in Fig. 2, permitted us to evaluate the system without introducing the variable attenuators, which had not yet been fully integrated. The 800-nm source beam was attenuated to a mean power of $\sim 20 \text{ mW}$ at the surface of the phantom, and data were collected for 60 s at each source position at count rates of $\sim 2.5 \times 10^4$ to 2.5×10^5 photons/s, depending on the position of the detector fiber relative to the source. The variability in absolute temporal delay owing to different lengths of source fibers and detector bundles was precalibrated, and the 256 acquired temporal point-spread functions were adjusted accordingly.

For the experiment, two data types were derived from each temporal point-spread function: the mean flight time and the variance about the mean. To reduce the influence of a minor systematic artifact in

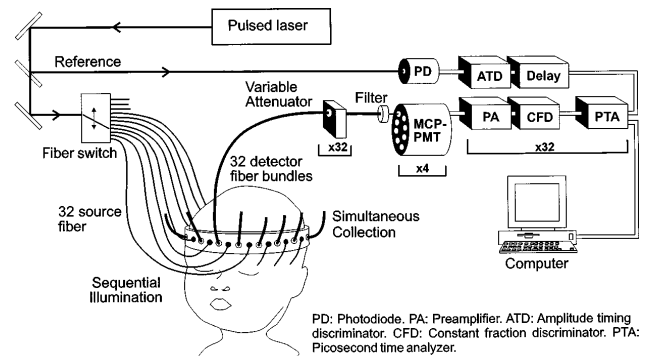


Fig. 1. 32-channel time-resolved imaging system.

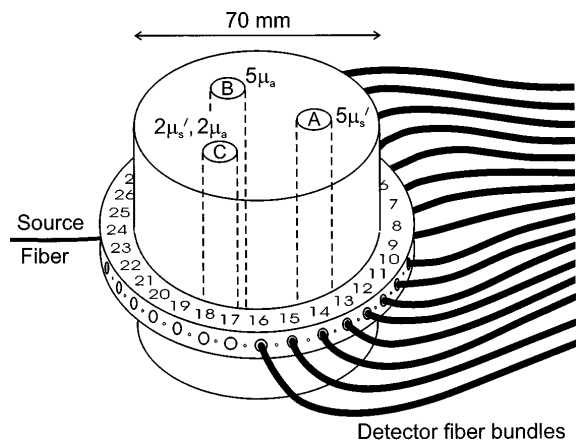


Fig. 2. Solid tissue-equivalent phantom and the fan-beam acquisition geometry.

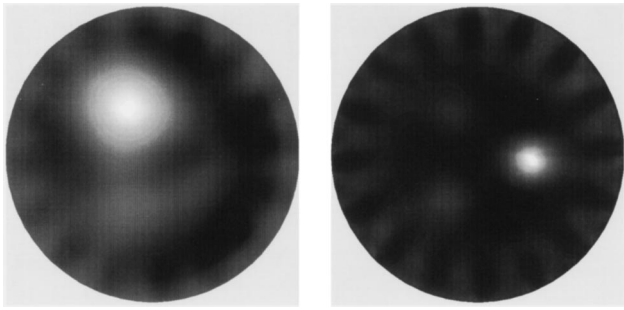


Fig. 3. Reconstructed maps of absorption (left) and scatter (right).

the data that was due to multiple reflection in the detector optics, we calculated the variance from a diffusion model fit to the data rather than from the data themselves.¹⁴ Then, using the coordinates of the surface location of every source and detector and an appropriate finite-element method mesh (consisting of 7392 triangular elements) describing a uniform circular cross section of the phantom, we employed the TOAST algorithm to derive simultaneous maps of the absorbing and the scattering properties. We used the nonlinear conjugate-gradient method with median filtering after each update.¹¹ We obtained the initial guess by first globally fitting homogeneous μ_a and μ_s' values to all the data. Although TOAST embodies several Bayesian regularization schemes, we did not employ any here, since such schemes are highly dependent on prior choice of hyperparameter and we wish to demonstrate the raw quality of the data. Instead, the stopping condition of the iterative scheme can be considered a regularization. Reconstruction required ~ 15 s per iteration on a Pentium PC.

The symmetry of the phantom and the confinement of the sources and the detectors to a single plane enabled TOAST to employ a 2D forward model, which resulted in a considerable reduction in computation time compared with that of 3D models. Although previous work¹⁵ has shown that intensity measurements acquired in three dimensions give rise to artifacts in a 2D reconstruction, unless appropriate data processing based on a calibration object is carried out, the use of purely temporal (and self-normalized) measurements significantly reduces the artifacts.

The results obtained after 30 iterations, after which no noticeable improvement was observed, are shown in Fig. 3. Qualitative agreement with the known locations and properties of the three regions shown in Fig. 2 is remarkably good. The absorption map is dominated by region B, whereas the scattering map clearly indicates the highly scattering region A and the smaller contrast of region C. The inherent spatial resolution of the absorption map is somewhat inferior, owing to the relatively weak dependence of both data types on absorption compared with their dependence on scatter.

Despite the relative simplicity of the phantom employed for this experiment, the results represent a highly significant step toward a clinical implementation of optical tomography. We have established that

it is possible to obtain time-resolved data quickly and reliably with a multichannel system and to acquire separate maps of the internal absorption and scattering properties without recourse to measurements that depend on intensity or to a reference or calibration measurement. Although the results presented here are strictly qualitative, means of extracting accurate absolute values of the reconstructed parameters are being investigated. The MONSTIR is currently being evaluated in a fully automated 32-channel configuration (32 detector bundles and 32 source fibers), resulting in a fourfold increase in data-collection efficiency and obviating the need for manual rotation. A 3D forward model for TOAST is being optimized, and means of including nonscattering regions are being introduced. Investigations are being performed of the effectiveness of various combinations of data type for simultaneous reconstruction, and their susceptibility to various sources of noise is being evaluated. Testing of complex tissuelike phantoms is already in progress, and experiments on clinical subjects will follow.

Judging the relative merits of different instruments and reconstruction software is difficult without comparative experimental cases. Therefore we have made our data, phantoms, and software available at the website of the UCL Biomedical Optical Research Group (www.medphys.ucl.ac.uk/research/borg).

Support for this research has been generously provided by the Wellcome Trust.

References

1. B. Chance and R. R. Alfano, eds., Proc. SPIE **2979**, (1997).
2. S. R. Arridge and J. C. Hebden, Phys. Med. Biol. **42**, 841 (1997).
3. S. R. Arridge and M. Schweiger, "A general framework for iterative reconstructive algorithms in optical tomography using a finite element method," in *Computational Radiology and Imaging: Therapy and Diagnosis*, C. Borgers and F. Natterer, eds., Vol. 110 of IMA Volumes in Mathematics and Its Applications (to be published).
4. M. Schweiger, S. R. Arridge, and D. T. Delpy, J. Math. Imag. Vision **3**, 263 (1993).
5. H. Jiang, K. D. Paulsen, U. L. Osterberg, B. W. Pogue, and M. S. Patterson, Opt. Lett. **20**, 2128 (1995).
6. H. Jiang, K. D. Paulsen, U. L. Osterberg, and M. S. Patterson, Med. Phys. **25**, 183 (1998).
7. B. W. Pogue, M. S. Patterson, H. Jiang, and K. D. Paulsen, Phys. Med. Biol. **40**, 1709 (1995).
8. S. R. Arridge and M. Schweiger, Opt. Express **2**, 213 (1998), www.osa.org.
9. S. R. Arridge, Appl. Opt. **34**, 7395 (1995).
10. M. A. O'Leary, D. A. Boas, B. Chance, and A. G. Yodh, Opt. Lett. **20**, 426 (1995).
11. S. R. Arridge and W. R. B. Lionheart, Opt. Lett. **23**, 882 (1998).
12. Y. Ueda, K. Ohta, M. Oda, M. Miwa, Y. Yamashita, and Y. Tsuchiya, Jpn. J. Appl. Phys. **27**, 2717 (1998).
13. K. Wells, J. C. Hebden, F. E. W. Schmidt, and D. T. Delpy, Proc. SPIE **2979**, 599 (1997).
14. J. C. Hebden and D. T. Delpy, Opt. Lett. **19**, 311 (1994).
15. M. Schweiger and S. R. Arridge, Appl. Opt. **37**, 7419 (1998).